رؤى جديدة في تحسين تأثير التوصيل للمنطقة
المسدودة في خزان الغاز الضيق المكسور

جيبينغ هي* ، ** ، هاو تشانغ* ، ** ، **** ، منغجينغ شاو* ، تشاو ران* وزانغوليان ***

* كلية الطاقة، جامعة تشنغدو للتكنولوجيا، تشنغدو، سيتشوان، جمهورية الصين الشعبية، 610059

** مختبر مفتاح الدولة للنفط وجيولوجيا غاز الخزان والاستغلال (جامعة تشنغدو من تيشنولوغي)، تشنغدو، سيتشوان، جمهورية الصين الشعبية، 610059

*** مختبر مفتاح الدولة للنفط وجيولوجيا غاز الخزان والاستغلال في جنوب غرب البترول، جامعة تشنغدو، سيتشوان، جمهورية الصين الشعبية، 610500

**** الاتصال مع المؤلف بالبريد الإلكتروني: cdutzhh08@163.com (هاو تشانغ)

الخــلاصــة

فقدان الدورة هو واحد من المشاكل التي تعوق الحفر الآمن والسريع في خزان الغاز الضيق المتكسر. واستنادا إلى المحاكاة العددية وتجارب التوصيل، تم اقتراح أفكار جديدة حول تحسين تأثير التوصيل في هذه الورقة. تم تقسيم الكسر إلى كسر الفم، كسر ضيق، وكسر طرف. تم تقييم مناطق التوصيل التي شكلت في كسر الفم وكسر ضيق، على التوالي. أظهرت نتائج التجارب أن تأثير التوصيل في هذين الموضعين مختلف. وكان متوسط MPP (أقصى ضغط التوصيل) من منطقة التوصيل التي شكلت في فم كسر هو 5.2 ميجاباسكال فقط، ولكن قيمة MPP المتوسطة لمنطقة التوصيل تشكلت في كسر ضيق يمكن أن تصل إلى أكثر من 9.2 ميجاباسكال. علاوة على ذلك، لنصل الى نفس قيمة MPP، توصيل عند المنطقة الضيقة المكسورة محتاجة اقل مواد دورة مفقودة (LCMs) واقل فقد للسوائل بالمقارنة مع التوصيل عند كسر الفم. هذا العمل يبين أن التوصيل عند كسر ضيق ممكن يحصل على توصيل أحسن من التوصيل عند الفم المكسور والذي تم اثباته في مجال (HB) في شمال شرق حوض سيشوان.

New insights into improving the plugging effect of plugging zone in fractured tight gas reservoir

Jiping She*, **, Hao Zhang*, **, ****, Mengjing Shao*, Chao Ran* and Zhanghua Lian***

*College of Energy, Chengdu University of Technology, Chengdu, Sichuan 610059, China

** State Key Lab of Oil and Gas Reservoir Geology and Exploitation (Chengdu University of Technology), Chengdu, Sichuan 610059, China

*** Southwest Petroleum University, Chengdu, Sichuan 610500, China

****Corresponding Author: zhanghao@cdut.edu.cn (Hao Zhang)

ABSTRACT

Lost circulation is one of the problems that impede safe and fast drilling in fractured tight gas reservoirs. Based on the numerical simulation and plugging experiments, new insights into improving the plugging effect were proposed in this paper. Fracture was divided into fracture mouth, fracture narrow, and fracture tip. Plugging zones were evaluated, which formed at the fracture mouth and fracture narrow, respectively. Experiments' results showed that the plugging effect at these two positions is different. The average maximum plugging pressure (MPP) of the plugging zone formed at fracture mouth was only 5.2MPa, but the average MPP of the plugging zone formed at the fracture narrow could reach more than 9.2MPa. Moreover, to reach the same MPP, plugging at fracture narrow needed less lost-circulation materials (LCMs) and lower fluid loss compared with plugging at fracture mouth. This work indicates that plugging at fracture narrow can get a better plugging effect than plugging at fracture mouth, which has been successfully confirmed in the HB field in northeast Sichuan Basin.

Keywords: Fractured reservoir; lost circulation; fracture narrow; plugging effect; plugging pressure.

INTRODUCTION

Lost circulation can seriously hinder the exploration and development of oil and gas resources. An American Petroleum Institute study published in 1991 includes data indicating that up to 45% of all wells require an intermediate casing string to prevent severe lost circulation while drilling to total depth. Some are as reported many more occurrences of lost-circulation events ranging from 40% to 80% of wells due to developed fractures (Yang, 2011; Xu *et al*., 2014; Arshad *et al*., 2014). The same as Northeast Sichuan Basin, low strength of rock, high development of fracture, and poor plugging ability of drilling fluid often lead to wellbore break down and natural and induced fracture propagation (Fig. 1). In the case of occurrences of natural and induced fractures, in which drilling-fluid density is already minimized or cannot be altered, improving plugging effect of drilling fluid is often used for strengthening wellbore and preventing lost circulation by using some LCMs.
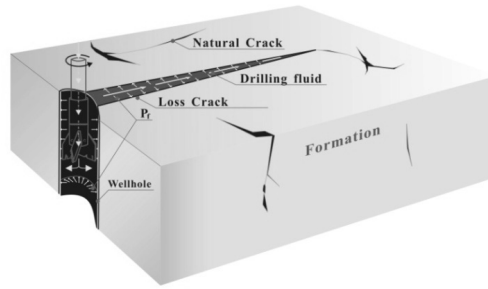
Figure 1. 3D model of lost circulation.

It is well known that fracture width variation is a key parameter used to design sizes of LCMs. At present, there are two most commonly used methods to get the fracture width variation. One is that fracture width variation is calculated according to the lost circulation parameters. In this method, based on the diffusion equation, fracture width variation model can be established by considering the net pressure, loss rate, volume and time (Sanfillippo *et al*., 1997). Another model is that fracture width variation is calculated directly using mechanical parameters, including in situ stress, rock strength (Wang *et al*., 2008), crustal stress (Whitfill *et al*., 2008), and fracture deformation characteristic (Li *et al*., 2014). Fracture width could be generally achieved by establishing a mathematical model (Tran *et al*., 2013) or numerical simulation (Alberty and McLean, 2004; Xu *et al*., 2014). However, previous investigations generally considered the fracture as parallel plane fracture and ignored the fracture width variation in length direction.

Apart from calculating fracture width variation, the plugging effect of plugging zone are also correlated to the type and strength of LCMs, plugging position and so on (Xu *et al*., 2014; Kang *et al*., 2014). Generally speaking, rigid particles are indispensable component in LCMs and frequently used as bridging materials in the process of plugging (Li, 2011). In addition, combinations of LCMs (e.g., combination of rigid particles and fiber materials) work more effectively compared to using only one type of LCMs (Kefi *et al*., 2010; Xu *et al*., 2014; Savari *et al*., 2014). In the process of plugging, the fiber materials can fill the space between granular materials and increase impermeability and friction of the plugging zone (Amanullah *et al*., 2006; Bassey *et al*., 2012; Mehdi *et al*., 2010; Arlanoglu *et al*., 2014), which can greatly improve MPP of the plugging zone. In addition, plugging position in fracture has significant influence on the MPP. If rigid particles bridge at the fracture mouth, the plugging zone is easy to be destroyed due to the increasing of tangential stress, while, bridging inside the fracture, the plugging zone becomes more stable (Mehdi *et al*., 2010). However, the problem on plugging-position selection was less studied in the previous work.

This study takes fractured tight gas reservoir of HB field in northeast Sichuan Basin as the object In this field, pore pressure gradient is 1.65MPa/100m, vertical stress gradient is 2.55MPa/100m, maximum horizontal stress gradient is 3.01MPa/100m and minimum horizontal stress gradient is 1.91MPa/100m.In the drilling process of this field, lost circulation is the most common down hole complex problem (Yang, 2011). The main factors were developed: vertical fracture, high positive pressure (wellbore pressure was 5 to 8 MPa over the pore pressure) and low MPP of plugging zone. We simulated the fracture width variation under different net pressures by using ABAQUS

finite element software and designed experiments to evaluate plugging effects of plugging zones. New insights into improving the plugging effect of plugging zone were proposed according to the fracture width variation and evaluation results of experiments.

FRACTURE WIDTH VARIATION SIMULATION

Simulation method

Based on the developed characteristics of fractures, we established a quarter-symmetry finite element model (Fig. 2), whose size was 12×8 m. In this model, arc FA stood for the wellbore, line segment AB represented a vertical fracture, and line segment BC and EF were symmetry constraints. The maximum horizontal stress P1 was loaded on the line segment CD, and the minimum horizontal stress P2 was loaded on the line segment DE. There are five assumptions of this model. Rock was isotropic porous media and elastic deformation body. Fracture surface was plane. The impacts of filtration and temperature were neglected. Input parameters of model were shown in Table 1.
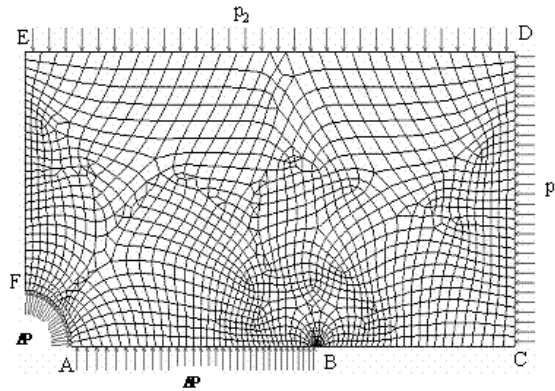

Figure2. A quarter FEM model of single vertical fracture.

Table 1. Input parameters of the model.

Young's modulus	6x103 MPa	Minimum horizontal stress	38MPa	Pore pressure	33MPa
Poisson's ratio	0.25	Permeability	0.05mD	Time	100s
Cohesion	30MPa	Tensile strength	4.7 MPa	Wellbore radius	0.1m
Vertical stress	51MPa	Biot coefficient	0.35	Total compressibility	2x 10^{-6} 1/MPa
Maximum horizontal stress	60MPa	Fracture half-length	1m	Internal friction angle	30°

According to the positive pressure range of drilling process, the net pressure ranged from 1 to 3MPa. Based on the formula in Appendix A and data in Table 1, stress intensity factors could be calculated under this net pressure condition. Critical stress intensity factor (K_{IC}) was 10.12 MPa*m$^{1/2}$. When the net pressure was 3MPa, the stress intensity factor in the fracture tip (K_I) was 9.33 MPa*m$^{1/2}$, less than

the critical stress intensity factor (K_{IC}), which indicates that the fracture cannot propagate in length direction. So, this study did not consider fracture extension.

Simulation results

Simulation results were shown in Fig.3. It showed that higher net pressure induced larger fracture width. The fracture-width increment of fracture mouth was the greatest compared with other positions. Fracture width gradually decreased along the fracture length direction and reduced to zero at the fracture tip. In addition, the fracture width was calculated by analytical models in Appendix B and then compared with the simulation results. As shown in Fig.4, under the same net pressure and time, the simulation results were consistent with the analytical results. But, for the fracture width of fracture mouth, simulation results were greater than the analytical results. The main reason of this discrepancy was that the analytical results did not consider the influence of the non-uniformity of horizontal principal stress on the fracture width variation (Alberty and McLean, 2004).
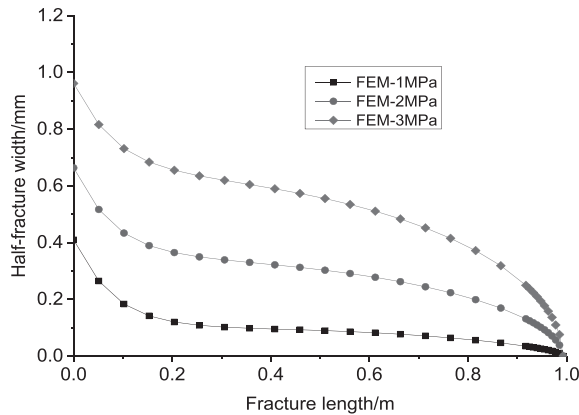

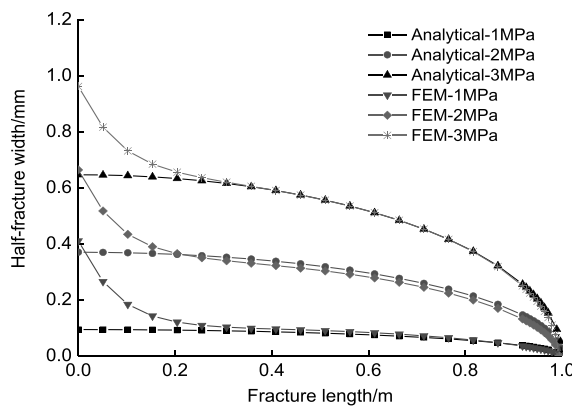**Figure 3.** Fracture width variations with different net pressures.

Figure 4. Fracture width variations of simulation and analytical results.

According to the simulation results, we found that the fracture looked like a wedge (Fig.5). And along the fracture length direction, the maximum width was at the fracture mouth, which

was represented by "*wmax*". The middle part of the fracture was narrower than the fracture mouth and was defined as "fracture narrow". The fracture width of the fracture narrow was represented by "w_{narrow}". The width of the fracture tip was zero. The difference widths of the fracture mouth and fracture narrow might provide a new solution to prevent lost circulation. In previous studies, designing the size of the LCMs generally was based on the "w_{max}" rather than the "w_{narrow}", which indicates that the case based on the "w_{max}" needs larger size particles to bridge in fracture. In fact, the size of LCMs can be optimized according to the widths of fracture mouth and fracture narrow. Moreover, the MPPs of plugging zones in the fracture mouth and fracture narrow might be different due to different fracture widths. So, it was necessary to evaluate the plugging effects of plugging zones at fracture mouth and fracture narrow by some experiments, respectively.
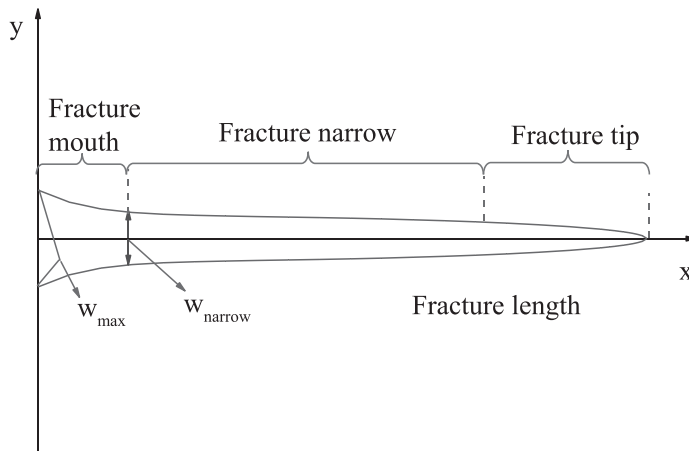

Figure5. A schematic diagram of a fracture and its components.

PLUGGING EXPERIMENTS EVALUATION

Samples and experimental method

Fractured plungers. To evaluate the plugging effects of plugging zones at fracture mouth and fracture narrow separately, we designed four metal plungers, including plungers A, B, C and D. Among them, A and C were plungers with straight fracture, while B and D were plungers with wedge fracture. Detailed geometrical parameters of them were shown in Table 2 and Fig. 6. For the plungers with wedge fracture, we could not determine whether the plugging zone formed in the fracture mouth or fracture narrow. So, the straight-fracture plungers A and C, instead of the wedge-fracture plunger B and D, respectively, were used to evaluate the plugging effects of plugging zones at fracture mouth.
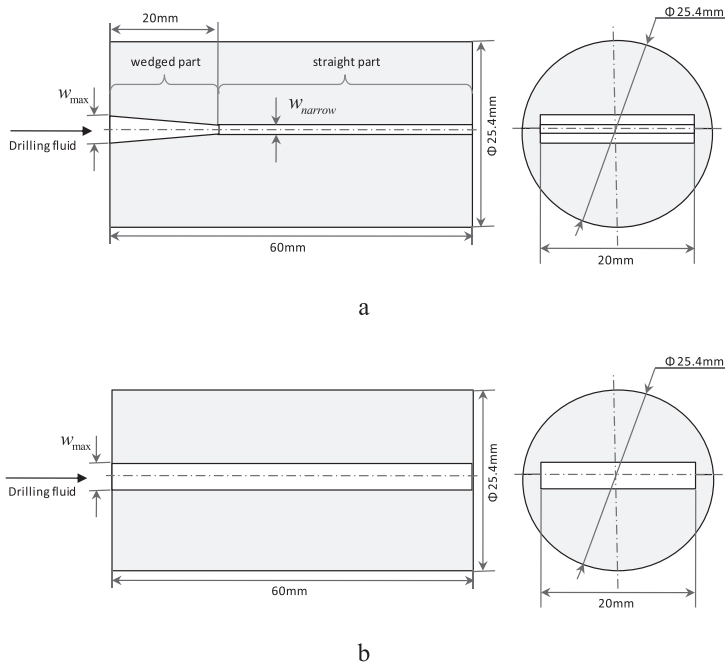
Figure 6. Metal plunger design schematics. (a) Wedge fracture. (b) Straight fracture.

Table 2. Fracture width design of metal plungers.

Sample number	Fracture type	w/mm	
		Fracture mouth（W_{max}）	Fracture narrow（W_{narrow}）
A	Straight fracture	1	1
B	Wedge fracture	1	0.5
C	Straight fracture	2	2
D	Wedge fracture	2	1.5

LCMs. As shown in Fig.7, LCMs had two types. One was rigid particle, and the other was fibrous materials. SRD, a kind of the rigid bridging particles, did not dissolve in water. Its main component was calcium carbonate, with an acid-soluble rate greater than 90%. Based on the proportional relation between the size of rigid bridging particles and the fracture width (0.6 w≤d≤1.0 w) (Li *et al*., 2011; Yan *et al*., 2012), four different size SRDs were used in the plugging experiments of plungers A, B, C and D, respectively. DTR and QP-1 were fibrous materials. The main components of DTR were low density micro-porous powders (granular) and soft fibrous materials. The lengths of the fibers ranged from 1 to 4mm. The acid-dissolution rate of DTR was about 36%.QP-1, a natural fiber material, had an acid-soluble rate of 90%.

Figure7. Three kinds of plugging materials.

Drilling fluid. Water-based drilling fluid was used in this study. Table 3 showed the formulation and properties of this drilling fluid. Taking the above three LCMs, twelve different drilling fluids were formulated, numbered F-1, F-2, F-3 and so on. Each kind of drilling fluid contained 3% DTR and 4%QP-1. For each size of the SRD particles, the concentrations in the drilling fluid were 1%, 2% and 3%, respectively. These twelve kinds of fluids were mixed completely in experiments.

Table 3. Formulation and properties of drilling fluid.

Bentonite (wt %)	K-PAM (wt %)	HV-CMC (wt %)	AV (mPa.s)	PV (mPa.s)	YP (Pa)	API-FL* (ml)	pH
6	0.5	1.0	75	24	51	10	9.5
*API-FL=fluid loss under standard API test conditions in cm^3							

Experimental method. Lost circulation evaluation apparatus was used in this experiment (Fig.8). The lost circulation evaluation apparatus is mainly composed of a kettle body, a core holder, a drilling fluid stirring device, and a data recording system. The kettle body is connected to the core holder. In the experiment, the drilling fluid in the kettle body is continuously stirred to prevent the sinking of the plugging material. The nitrogen pressure-driven drilling fluid was lost into the fracture core in the holder. The data recording system can record the plugging pressure and the loss of drilling fluid in the process of lost circulation. The experimental plan was shown in Table 4. The experimental procedures were as follows.
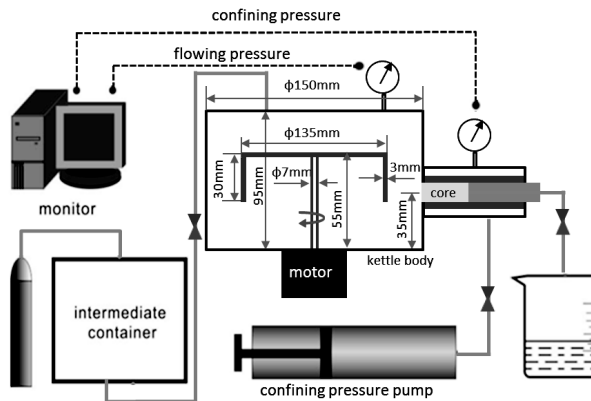

Figure 8. Schematic diagram of lost circulation evaluation apparatus.

Table 4. Experimental plan of plugging experiment.

Plunger	Fracture type	Plugging position	w /mm		Drilling fluid		
			w_{max}	w_{narrow}	Number	c(SRD)/%	d (SRD)/mm
A	Straight fracture	fracture mouth	1	1	F-1	1	0.8-1.0
					F-2	2	
					F-3	3	
B	Wedge fracture	fracture narrow	1	0.5	F-4	1	0.4-0.5
					F-5	2	
					F-6	3	
C	Straight fracture	fracture mouth	2	2	F-7	1	1.6-2.0
					F-8	2	
					F-9	3	
D	Wedge fracture	fracture narrow	2	1.5	F-10	1	0.9-1.1
					F-11	2	
					F-12	3	

"c"and "d" _Concentrationand size of SRD bridging particlesrespectively.

(1) Put plunger A into the core holder, increasing the confining pressure to 15MPa and remaining unchanged;

(2) Add 1.4L drilling fluid F-1 to the kettle of the lost circulation evaluation apparatus;

(3) Seal the kettle and turn on the agitating device (100r/min). Pressures in kettle were set at 3.5 MPa, 4MPa, 4.5MPa, 5MPa, 5.5MPa, 6MPa, 6.5MPa, 7MPa, 7.5MPa, 8MPa, 8.5MPa, 9MPa, 9.5MPa and 10MPa. Each pressure remained for 10min;

(4) Measure loss amount at the outlet under different pressures. If the cumulative loss amount reached 1L, the plugging was considered to be invalid, and then the experiment is stopped. The previous pressure was the MPP of plugging zone. Each experiment was repeated three times;

(5) Other drilling fluids and the plungers were evaluated using the same experimental procedure.

RESULTS AND DISCUSSION

The experimental results were shown in Table 5. According to the two plugging positions in fracture, we discussed two cases.

Case one: plugging the fracture mouth. The experimental results were shown in Fig. 9 and Fig. 11. In the experiment of plunger A, the concentration of the SRD bridging particles was increased from 1% to 3%, MPP increased correspondingly from 4MPa to 6.5MPa, and the cumulative loss ranged from 280 to 630 ml. In the experiment of plunger C, due to greater fracture width, when the concentration of the SRD bridging particles was 1% or 2%, the MPP was only 3.5MPa, and the cumulative loss ranged from 650 to 1000ml.When the concentration of SRD bridging particles was raised to 3%, the MPP increased to 8.5MPa, and the cumulative loss ranged from 328 to 393 ml.
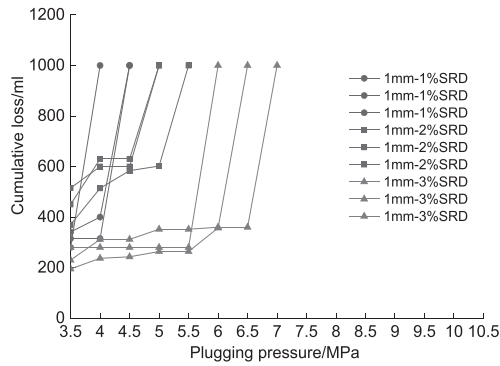
Figure 9. Plugging pressure and cumulative loss of sample A (w_{max} =1mm).
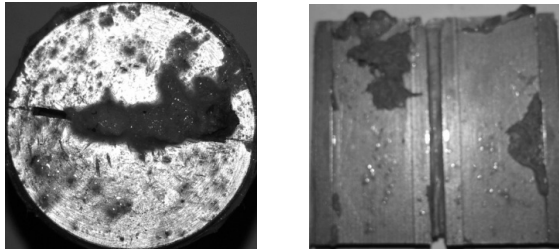
Figure 10. Plugging zone of fracture mouth (w_{max}:1mm, SRD:3%, MPP:5MPa).
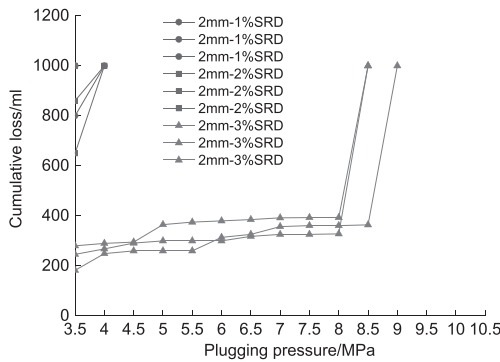
Figure 11. Plugging pressure and cumulative loss of sample C(w_{max} =2mm).

Figure 12. Plugging zone of fracture mouth (wmax: 2mm, SRD: 1%, MPP: 0MPa).

Besides, as shown in Fig. 10 and Fig. 12, In the process of loss, the SRD bridging particles and fibers formed merely a plugging zone at the fracture mouth, and the plugging zone was comparatively unsubstantial. Due to the increasing pressure and scouring of drilling fluid, the

plugging zone was easy to be destroyed, resulting in loss of circulation again. Greater fracture width made these effects more obvious.

Case two: plugging the fracture narrow. The experimental results were shown in Fig. 13 and Fig. 15. In the experiment of plunger B, when the concentration of SRD bridging particles was increased from 1% to 3%, MPP can reach 10MPa or more, and the cumulative loss was less than 10ml. In the experiment of plunger D, when the concentration of SRD bridging particles was 1%, the corresponding MPP is 5MPa, and the cumulative loss ranged from 400 to 600ml.When the concentration of SRD bridging particles was 2% and 3%, MPP could also reach10MPa, and the cumulative loss ranged from 425 to 487 ml, 341 to 440ml, respectively.

Figure 13. Plugging pressure and cumulative loss of sample B(w_{narrow}=0.5mm).

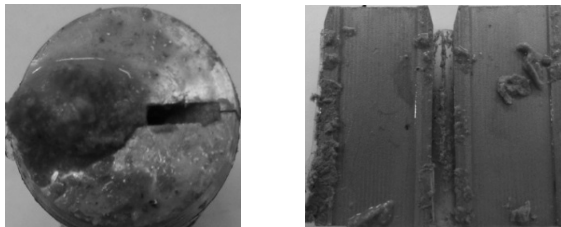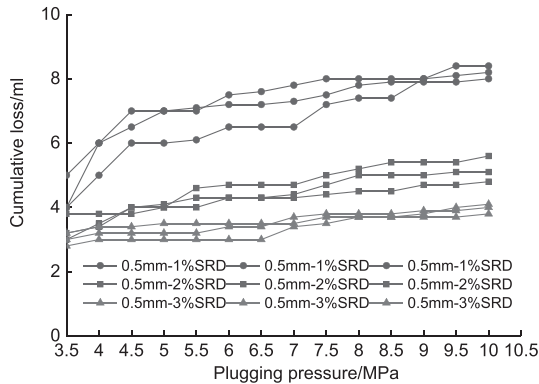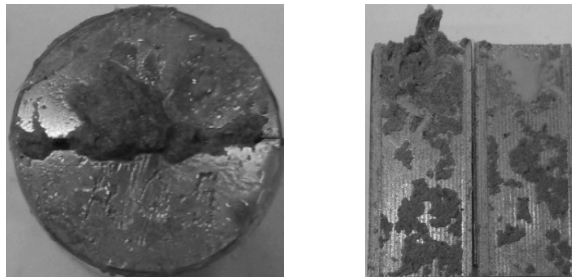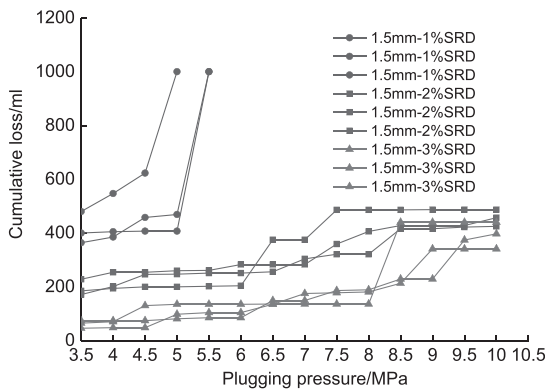**Figure 14.** Plugging zone between fracture mouth and fracture narrow (wnarrow: 0.5mm, SRD: 3%, MPP: ≥10MPa).

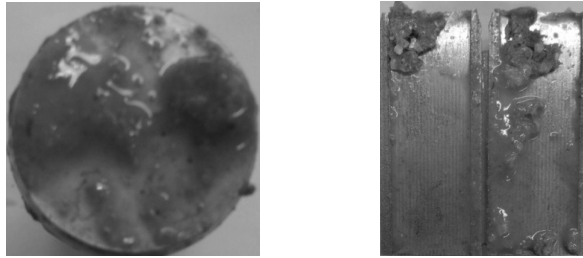**Figure 15.** Plugging pressure and cumulative loss of sample D (w_{narrow}=1.5mm).

Figure 16. Plugging zone between fracture mouth and fracture narrow (w_{narrow}: 1.5mm, SRD: 2%, MPP: ≥10MPa).

As shown in Fig. 14 and Fig. 16, it could be seen that there were four reasons to the case of plugging the fracture narrow. (1) The bridging particles and fibers formed a plugging zone at the fracture narrow and increased the flow resistance of drilling fluid. (2) Xu *et al*. studied the influencing factors of the MPP by plugging experimental. Experimental results indicate that rigid granule is important to the maximum plugging pressure; fiber plays an important role in improving plugging efficiency and reducing plugging zone permeability. The combination of rigid granule and fiber can create a synergistic effect to optimize fracture plugging effect (Xu *et al*., 2016). So, the synergistic effect of bridging particles and fibers can generate higher MPP. (3) The stage-by-stage filling effect between the fracture mouth and the fracture narrow could form a tight plugging zone, so the plugging zone was difficult to be destroyed. (4) This plugging zone was formed inside the fracture rather than fracture mouth near the wellbore, which implied that the former was almost not affected by the scouring of drilling fluid.

In conclusion, when the concentration of bridging particles was increased from 1% to 3%, the MPP increased, and the cumulative loss decreased gradually. As shown in Table 5, the average MPP of plugging zone at fracture mouth was only 5.2MPa, but the average MPP of plugging zone at fracture narrow could reach more than 9.2MPa. Moreover, to reach the same MPP, plugging at the fracture narrow required less LCMs and showed a lower fluid loss compared with plugging at the fracture mouth.

As we could conclude from the above analyses, this study offered some theoretical support for the design of plugging approach in the drilling process.

(1) Previous plugging designs were almost based on the maximum width of fracture mouth and regarded fracture width as a constant value, without considering the fracture width variation and different plugging positions. In fact, the width is a dynamic value with the changing of net pressure. And, plugging zones formed at different positions have different MPPs. So, when determining the plugging plan, we should take full account of the fracture width variation, plugging position and other parameters such as the bridging particle's size, concentration and gradation.

(2) Regarding high stress sensitivity fractured tight gas reservoir, once the drilling fluid flows into fracture, the rock of fracture surface is soaked in the drilling fluid. This process will reduce the strength of asperities on fracture surface, and then induce fracture stress sensitivity (He *et al*., 2012). This plugging approach can form a tough plugging zone at the fracture mouth and reduce the cumulative loss of drilling fluid in the process of drilling.

FIELD APPLICATION

For Well H-X (located in HB field in Northeast Sichuan Basin) drilled with water-based drilling fluid, serious lost circulations of 1.82-g/cm³ drilling fluid were observed at the FXG target formation. According to the parameters of pump pressure, pore pressure, and the in situ stress, the widths of fracture mouth and fracture narrow were calculated by the finite element method and were 1.05mm and 0.61mm, respectively. A solution that included 3% rigid particles (800~1000μm, the design of size was based on the width of fracture mouth) and 2% fiber (DTR and QP-1) was pumped into the loss zone. Results indicated that MPP of plugging zone was less than 6 MPa, and lost circulation occurs again when drilling continued. Then, 33-m³ new solution was pumped into the loss zone again, which included 2% rigid particles (400~600μm, the design of size was based on the width of fracture narrow) and 2% fiber (DTR and QP-1). Lost circulation was controlled after 30 min. The MPP of plugging zone was more than 10MPa and remained effective until the well was completed.

Table 5. Experimental results of plugging experiment.

Plunger	Fracture type	Plugging position	w/mm w_{max}	w/mm w_{narrow}	Drilling fluid	3.5	4	4.5	5	5.5	6	6.5	7	7.5	8	8.5	9	9.5	10
A	Straight fracture	Fracture mouth	1	1	F-1	Yes	Yes	No											
					F-2	Yes	Yes	Yes	Yes	No									
					F-3	Yes	Yes	Yes	Yes	Yes	Yes	Yes	No						
B	Wedge fracture	Fracture narrow	1	0.5	F-4	Yes	Yes	Yes	Yes	Yes	Yes	Yes	Yes	Yes	Yes	Yes	Yes	Yes	Yes
					F-5	Yes	Yes	Yes	Yes	Yes	Yes	Yes	Yes	Yes	Yes	Yes	Yes	Yes	Yes
					F-6	Yes	Yes	Yes	Yes	Yes	Yes	Yes	Yes	Yes	Yes	Yes	Yes	Yes	Yes
C	Straight fracture	Fracture mouth	2	2	F-7	Yes	No												
					F-8	Yes	No												
					F-9	Yes	Yes	Yes	Yes	Yes	Yes	Yes	Yes	Yes	Yes	Yes	No		
D	Wedge fracture	Fracture narrow	2	1.5	F-10	Yes	Yes	Yes	Yes	No									
					F-11	Yes	Yes	Yes	Yes	Yes	Yes	Yes	Yes	Yes	Yes	Yes	Yes	Yes	Yes
					F-12	Yes	Yes	Yes	Yes	Yes	Yes	Yes	Yes	Yes	Yes	Yes	Yes	Yes	Yes

CONCLUSION

(1) According to some parameters including in situ stress, rock mechanics, and fracture geometry, fracture width variation can be obtained by simulation method. The fracture width is a dynamic value with net pressure change. The width of fracture mouth is bigger than that of fracture narrow due to the effect of non-uniformity of horizontal principal stress.

(2) Plugging at fracture narrow demonstrates a better plugging effect than plugging at fracture mouth in preventing lost circulation. The former makes the plugging zone obtain higher MPP, requires less LCMs, and shows a lower fluid loss.

(3) This work provides some insights into the design of plugging approach in the drilling process, for example, designing the size and type of LCMs, improving the plugging pressure, and reducing stress sensitivity, which has important significance to prevent lost circulation.

ACKNOWLEDGMENT

Appendix A --- Stress Intensity Factor

Taking superposition principle, the stress intensity factor of fracture tip can be obtained through drilling fluid loss data. As shown in Fig. A.1, the stress intensity factors generated by horizontal stresses and wellbore fluid column pressure can be calculated via Eq. (A. 1) and (A. 2), respectively, then Eq. (A. 3) was formulated to compute the composite stress intensity factor (Tada, H., 2000).
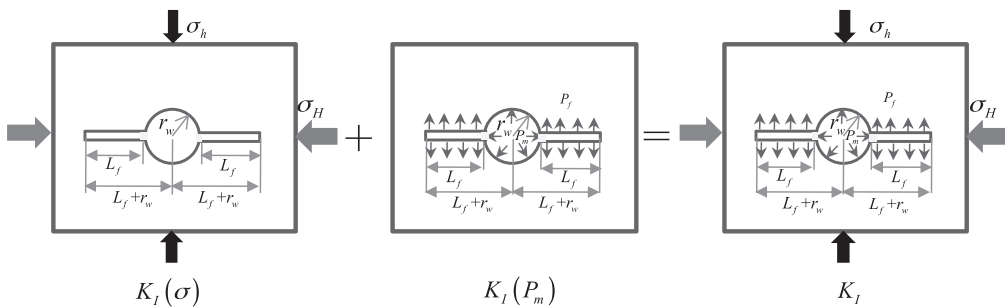

Fig. A.1. Single fracture stress intensity factor superimposed schematics.

$$K_I(\sigma_h) = -\sigma_h \sqrt{\pi L_f} F_\delta(s) \quad （A.1）$$

where

$$s = \frac{L_f}{L_f + r_w}$$

$$\delta = \sigma_H / \sigma_h$$

$$F_\lambda(s) = (1-\delta)F_0(s) + \delta F_1(s)$$

$$F_0(s) = 0.5 \times (3-s)\left[1 + 1.243(1-s)^3\right]$$

$$F_1(s) = 1 + (1-s)\left[0.5 + 0.743(1-s)^2\right]$$

$$K_I(P_m) = P_m \sqrt{\pi L_f} F_\omega(s) \quad （A.2）$$

where

$$\omega = P_f / P_m$$

$$F_\omega(s) = (1-\omega)F_0'(s) + \omega F_1(s)$$

$$F_0'(s) = (1-s)\left[0.637 + 0.485(1-s)^2 + 0.4s^2(1-s)\right]$$

$$K_I = K_I(\sigma_h) + K_I(P_m) \quad （A.3）$$

Since the drilling fluid-loss occurred in situ conditions, according to rock tensile strength and confining pressure parameters, rock critical intensity factor in situ conditions can be calculated by Eq. (A. 4) (Jin *et al*., 2001).

$$K_{IC} = 0.2176 P_c + 0.0059\sigma_t^3 + 0.0923\sigma_t^2 + 0.517\sigma_t - 0.3322 \quad （A.4）$$

where

$$P_c = \frac{\nu}{1-\nu}(P_v - \alpha P_p) + \alpha P_p$$

Appendix B ---Analytical Models of Fracture Width Variation

Without considering the temperature difference between fluid within the fracture and pore fluid, the basic equations of elastic mechanics in porous media can be expressed as the following forms (Settari and Mourits, 1998; Tran *et al*., 2012):

$$\varepsilon_{xx} = \frac{1}{E}[\sigma_{xx} - \nu(\sigma_{yy} + \sigma_{zz})] - \frac{\Delta p}{3H} \quad （B.1）$$

$$\varepsilon_{yy} = \frac{1}{E}[\sigma_{yy} - \nu(\sigma_{xx} + \sigma_{zz})] - \frac{\Delta p}{3H} \quad （B.2）$$

$$\varepsilon_{zz} = \frac{1}{E}[\sigma_{zz} - \nu(\sigma_{xx} + \sigma_{yy})] - \frac{\Delta p}{3H} \quad （B.3）$$

Where $H = \dfrac{1}{c_b - c_s} = \dfrac{1}{\alpha c_b} = \dfrac{K_b}{\alpha} = \dfrac{E}{3(1-2\nu)\alpha}$

Without considering the body force, the force-balance equations can be written as

$$\frac{\partial \sigma_{xx}}{\partial x} + \frac{\partial \tau_{xy}}{\partial y} = 0 \quad （B.4）$$

$$\frac{\partial \sigma_{yy}}{\partial y} + \frac{\partial \tau_{yx}}{\partial x} = 0 \quad （B.5）$$

Because of the conservation of momentum , solving Eq. (B. 4) with Eq. (B. 5) simultaneously will obtain

$$(\frac{\partial^2 \sigma_{xx}}{\partial x^2} + \frac{\partial^2 \sigma_{yy}}{\partial y^2}) = -2\frac{\partial^2 \tau_{xy}}{\partial x \partial y} \quad （B.6）$$

Model boundary conditions are as follows:

$$\sigma_{yy}(x,0) = p_f; 0 \leq x \leq c \quad （B.7a）$$

$$\sigma_{xx}(x,y) = S_0; \sqrt{x^2 + y^2} \rightarrow \infty \quad （B.7b）$$

$$\tau_{xy}(x,0) = 0; 0 \leq x \leq c \quad （B.7c）$$

$$\sigma_{yy}(x,y) = S_0; \sqrt{x^2 + y^2} \rightarrow \infty \quad （B.7d）$$

$$\tau_{xy}(x,y) = S_0; \sqrt{x^2 + y^2} \rightarrow \infty \quad （B.7e）$$

$$p(x,0) = p_f; 0 \leq x \leq c \quad （B.7f）$$

$$u(0,y) = 0; y \geq 0 \quad （B.7g）$$

$$v(x,0) = 0; x \geq c \quad （B.7h）$$

Through the deduction, the fracture width equation can be expressed as (Tran*et al*., 2012)

$$w(\eta) = \frac{2c \ (1-v^2)\sin\eta}{E}(P_f - \sigma_{yy}^h) \quad （B.8）$$

Here

$$\sigma_{yy}^h = \sigma_h + \frac{\lambda A_p}{1+2\lambda}(P_f - P_P) \quad （B.9）$$

By using the hyperbolic coordinates, the relation between x and η can be expressed as

$$\sin\eta = \sqrt{1 - (\frac{x}{c})^2} \quad （B.10）$$

Then, substituting " σ_{yy}^h " from Eq. (B. 9) and " $\sin\eta$ " from Eq. (B. 10) into Eq. (B. 8) leads to Eq. (B. 11):

$$w(x) = \frac{2(1-v^2) \ c\sqrt{1-(\frac{x}{c})^2}}{E}\left\{(P_f - \sigma_h) - \left[\frac{\lambda A_p}{1+2\lambda}\right](P_f - P_P)\right\} \quad （B.11）$$

Here, $A_p = \dfrac{E}{3(1-v)H} = \dfrac{\alpha(1-2v)}{1-v}, \lambda = \sinh^{-1}(\dfrac{\gamma_p}{c}\sqrt{\dfrac{\pi k t}{\phi \mu C_p}})$

Nomenclature

c =fracture half-length, m

c_b = bulk compressibility, 1/kPa

C_p =total compressibility, 1/kPa

d= Bridging particle size

E =Young's modulus, kPa

H =ratio of bulk modulus to Biot's coefficient

k =permeability, m^2

P_c =confining pressure in situ conditions, MPa

P_P =pore pressure, kPa

P_m =drilling fluid column pressure, MPa

P_f =fluid pressure within the fracture, MPa

t =time, seconds

u= horizontal displacement

v=vertical displacement

w =fracture-width, m

K_I =stress intensity factor, MPa*m$^{1/2}$

K_{IC} =critical stress intensity factor, MPa*m$^{1/2}$

σ_t =tensile strength, MPa

σ_h =the minimum horizontal principal stress, MPa

σ_H = the maximum horizontal principal stress, MPa

α =Biot's coefficient

ν =Poisson's ratio

λ =penetration depth for pressure in elliptical coordinates

γ_p =coefficient of penetration depth

ε =normal strain, m/m

μ =viscosity, kPa.s

σ =normal total stress, kPa

τ =shear stress, kPa

ϕ =porosity

Subscript

x, xx = x-direction

y, yy = y-direction

z, zz = z-direction

REFERENCES

Alberty, M. W. & McLean, M. R. 2004. A physical model for stress cages. SPE Annual Technical Conference and Exhibition, 26-29 September, Houston, Texas.

Amanullah, M. & Boyle, R. 2006. Experimental evaluation of formation-strengthening potential of a novel gel system. IADC/SPE Asia Pacific Drilling Technology Conference and Exhibition, 13-15 November, Bangkok, Thailand.

Arlanoglu, C., Feng, Y. & Podnos, E. 2014. Finite element studies of wellbore strengthening. IADC/SPE Drilling Conference and Exhibition, 4-6 March, Fort Worth, Texas, USA.

Bassey, A., Dosunmu, A. & Iorkam, A. 2012. A new (3D MUDSYST Model) approach to wellbore strengthening while drilling in depleted sands: a critical application of LCM and stress caging model. Nigeria Annual International Conference and Exhibition, 6-8 August, Lagos, Nigeria.

He, J. G., Kang, Y. L. & You, L. J. 2012. Effects of mineral composition and microstructure on stress-sensitivity of mud rocks. Natural Gas Geoscience, **23**(01):129–134.

Jin, Y., Chen, M. & Zhang, X.D. 2001. Determination of fracture toughness for deep well rock with geophysical logging data. Chinese Journal of Rock Mechanics and Engineering, **20**(04): 454-456.

Kang, Y. L., Xu, C. Y. & Tang, L. 2014. Constructing a tough shield around the wellbore: theory and method for lost-circulation control. Petroleum Exploration and Development, **41**(04): 520-527.

Kefi, S., Lee, J. C. Shindgikar, N. D., Brunet-Cambus, C., Vidick, B. & Diaz, N. I. 2010. Optimizing in four steps composite lost-circulation pills without knowing loss zone width. IADC/SPE Asia Pacific Drilling Technology Conference and Exhibition, 1-3 November, Ho Chi Minh City, Vietnam.

Li, J. X., Huang, J. J. & Luo, P. Y. 2011. Plugging mechanism and estimation models of rigid particles while drilling in fracture formations. ACTA PETROLEI SINICA, **32**(03): 509-513.

Li, S., Kang, Y. L. & You, L. J. 2014. Experimental and numerical investigation of multiscale fracture deformation in fractured–vuggy carbonate reservoirs. Arabian Journal for Science and Engineering, **39**(5): 4241-4249.

Mokhtari, M. & Ozbayoglu, M. E. 2010. Laboratory investigation on gelation behavior of xanthan cross linked with borate intended to combat lost circulation. SPE Production and Operations Conference and Exhibition, 8-10 June, Tunis, Tunisia.

Sanfillippo, F., Brignoli, M. & Santarelli, F. J. 1997. Characterization of conductive cracks while drilling. SPE European Formation Damage Conference, 2-3 June, The Hague, Netherlands.

Settari, A., &Mourits, F. M.1998. A coupled reservoir and geomechanical simulation system. SPE Journal, **3**(03): 219-226.

Hiroshi, T. & Paris, P. C. 2000. The analysis of cracks handbook. ASME Press, New York.

Tada, H., Paris, P., &Irwin, G. The analysis of cracks handbook. New York: ASME Press, 2000: 296-299.

Tran, D., Settari, A. T. & Nghiem, L. 2012. Predicting growth and decay of hydraulic-crack width in porous media subjected to isothermal and nonisothermal flow. SPE Canadian Unconventional Resources Conference, 30 October-1 November, Calgary, Alberta, Canada.

Wang, H., Sweatman, R. E. & Engelman, R. 2008. Best practice in understanding and managing lost circulation challenges. SPE Drilling & Completion, **23**(02): 168-175.

Whitfill, D. L., Jamison, D. E. & Wang, H. 2008. Lost circulation material selection, particle size distribution and crack modeling with crack simulation software. IADC/SPE Asia Pacific Drilling Technology Conference and Exhibition, 25‑27 August, Jakarta, Indonesia.

Xu, C. Y., Kang, Y. L. & You, L. J. 2014. High-strength, high-stability pill system to prevent lost circulation. Society of Petroleum Engineers.SPE Drilling & Completion, **29**(03):334‑344.

Xu, C. Y., Kang, Y. L., Chen, F. & You, Z. J. 2016. Fracture plugging optimization for drill-in fluid loss control and formation damage prevention in fractured tight reservoir. Journal of Natural Gas Science and Engineering, 35:1216‑1227.

Yan, F. M., Kang, Y. L. & Sun, K. 2012. The Temporary plugging formula for fractured-vuggy carbonate reservoir. Petroleum Drilling Techniques, **40**(1): 47‑51.

Yang Z. B. 2011. Engineering geology features and drilling strategy in Heba structure, northeast Sichuan. Dissertation, Chengdu University of Technology.